Optimal LED Selection for Multispectral Lighting Reproduction

Chloe LeGendre, Xueming Yu, Paul Debevec; USC Institute for Creative Technologies, Playa Vista, CA, USA

Abstract

We demonstrate the sufficiency of using as few as five LEDs of distinct spectra for color-accurate multispectral lighting reproduction and solve for the optimal set of five from 11 such commercially available LEDs. We leverage published spectral reflectance, illuminant, and camera spectral sensitivity datasets to show that two approaches of lighting reproduction, matching illuminant spectra directly and matching material color appearance observed by one or more cameras or a human observer, yield the same LED selections. Our proposed optimal set of five LEDs includes red, green, and blue with narrow emission spectra, along with white and amber with broader spectra.

Introduction

Lighting reproduction systems as in Debevec et al. [2] and Hamon et al. [6] surround a subject with red, green, and blue (RGB) light emitting diodes (LEDs), driving them to match a real-world lighting environment recorded using high dynamic range, panoramic RGB photography. A subject is thus illuminated as in Fig. 1 with a reproduction of the directions, colors, and intensities of light, appearing as they would in the actual scene into which they will later be composited. While compositing results can be convincing (especially after image manipulation by color correction artists), Wenger et al. [16] and LeGendre et al. [10] observed poor color rendition using only RGB LEDs for lighting reproduction. Color rendition is compromised because RGB LEDs lack energy at certain wavelengths across the visible light spectrum *and* the total emission spectrum of an RGB light source is confined to be a linear combination of each of the relatively narrow individual red, green, and blue LED emission spectra. As such, while RGB LEDs can produce light across a wide gamut of observable colors, they cannot reproduce light of any *spectrum*. Accordingly, material appearances under RGB LED reproduced lighting are unlikely to match those under the complex illumination environments of the real world.

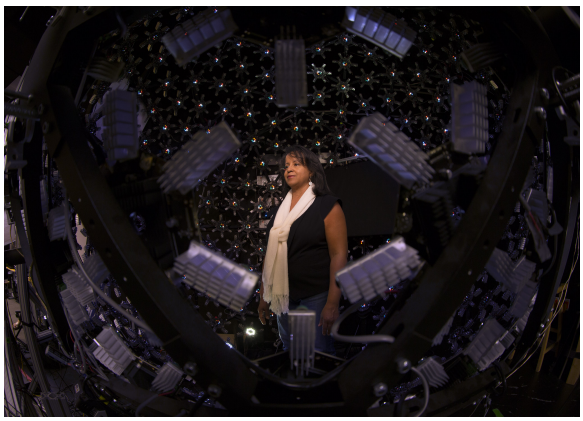

Figure 1. *Omnidirectional lighting reproduction.*

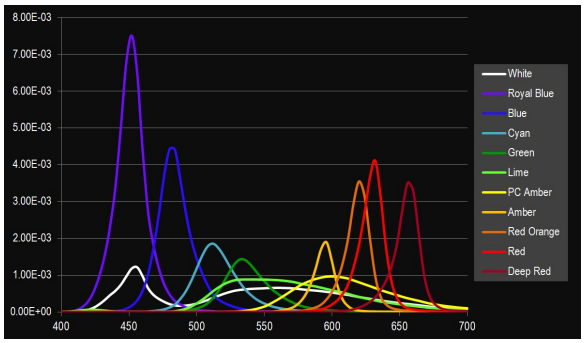

Figure 2. *Spectra of the 11 Lumileds Luxeon LEDs evaluated, corresponding to Royal Blue (Y), Blue (B), Cyan (C), Green (G), Lime (L), PC Amber (P), Amber (A), Red-Orange (O), Red (R), Deep Red (D), and White (W).*

Both Wenger et al. [16] and LeGendre et al. [10] extended lighting reproduction to the multispectral domain, considering light sources comprised of more than just RGB LEDs, for the single light source and omnidirectional lighting scenarios respectively. Intuitively, adding more individually-controllable spectral channels to a light source should improve its color rendition capability, but each additional spectral channel also adds complexity. As such, a minimal, sufficient set of LEDs may be of interest to visual effects practitioners and luminaire manufacturers. While both [16, 10] demonstrated improved color rendition when using more than just RGB LEDs, neither discussed a minimal, sufficient set of LEDs for multispectral lighting reproduction.

We approach the selection of such a set of LEDs by evaluating the color rendition capabilities of different LED combinations. We evaluate color matches for various materials of diverse reflectance spectra as viewed under different real-world illuminants by multiple observers. We find the optimal set of LEDs from an initial set of 11 commercially-available LEDs with distinct, visible light emission spectra. Along with white (W), we consider the 10 Lumileds Luxeon Rebel ES colors: Royal Blue (Y), Blue (B), Cyan (C), Green (G), Lime (L), PC Amber (P), Amber (A), Red-Orange (O), Red (R), and Deep Red (D) with spectra in Fig. 2. We first determine the number k of LEDs of distinct spectra such that adding an additional LED no longer meaningfully improves lighting reproduction, and we next determine the optimal subset of k such LEDs to use for reproducing diverse and complex illuminants.

We solve for a minimal, sufficient set of LEDs using two different approaches from Wenger et al. [16]: *Spectral Illuminant Matching* (SIM) and *Metameric Reflectance Matching* (MRM). With SIM, we compute a linear combination of individual LED emission spectra that best matches a target illuminant spectrum in a least-squares sense. With MRM, we compute a linear combination of individual LED emission spectra that best matches the appearance of a color chart as observed by one or more cameras,

or the standard human observer. From our analysis, our contributions are the following:

1. We show that using more than *five* LEDs of distinct spectra yields diminishing returns for color rendition in multispectral lighting reproduction, for the diverse illuminants, materials, and observers we consider.
2. We propose an *optimal* set of five LEDs which includes: red, green, and blue LEDs with narrow emission spectra, plus white and amber LEDs with broader emission spectra.

Related Work

Lighting Reproduction

In this work, we are interested in selecting a minimum, sufficient set of LEDs for a multispectral light source used to replicate a real-world lighting environment inside a studio, while ensuring good color rendition performance. As previously described, Debevec et al. [2] and Hamon et al. [6] reproduced omnidirectional lighting environments using only RGB LEDs, with computer-controllable light sources and LED flat panels respectively, but neither evaluated color rendition or optimized LED selection based on emission spectra.

Wenger et al. [16], seeking to cover the gaps between the emission spectra of RGB LEDs for a single light source, demonstrated improved color rendition for skin and the squares of a color chart when using a nine-channel multispectral light instead of an RGB source but did not discuss a minimal, sufficient LED set. As bright yellow LEDs were not then available, they filtered two white LEDs of their nine-channel source to produce dim yellow light. Although multispectral illumination can be achieved by selectively filtering broad spectrum white light, we consider this approach out of scope for our analysis since the overall quantity of light after filtering will be far lower for the same input power, although the same optimization approaches can be applied.

Fryc et al. [3] extended this work [16] to develop an LED-based spectrally-tunable light source using 35 LEDs of distinct spectra, evaluating *Spectral Illuminant Matching* (SIM) when trying to reproduce daylight, various fluorescent, and HMI illuminants. This work did not consider color rendition and did not discuss a minimal, sufficient LED set. However, both Wenger et al. [16] and Fryc et al. [3] noted the lack of available "yellow-green" LEDs, with emission spectra around 550 nm, at that time. Due to recent advances in solid state lighting, two new LEDs from Lumileds Lighting, the Luxeon Rebel ES colors Lime and PC Amber, now cover this spectral gap, but they are still dimmer than other LEDs, and they have broader emission spectra. Both consist of royal blue emitters with emission-broadening phosphors, each with essentially no remaining emitter output. Our current work evaluates the usefulness of these two newer emitters for multispectral lighting reproduction.

LeGendre et al. [10] reproduced omnidirectional lighting in a six-channel, multispectral light stage with RGB, cyan (C), amber (A), and white (W) LEDs. When using only RGBW LEDs, color rendition was improved for skin, the squares of a color chart, and various fabric samples, as compared with RGB-only lighting. Even closer color matches were achieved when using all six multispectral (RGBCAW) LEDs. However, the LED selection process was justified again as the covering of spectral gaps between the RGB LEDs. These works [16, 10] using LED sources with four, six, or nine spectral channels with improved color rendition over RGB-only lighting motivate our interest in finding a minimal, sufficient set of LEDs for multispectral lighting reproduction.

Multispectral Reflectance Capture

Spherical or dome-shaped multispectral LED lighting rigs have also been designed and constructed to illuminate a subject from all directions for the purpose of multispectral material reflectance measurement. The system of Ajdin et al. [1] used sixteen spectral channels, while that of Gu and Liu [5] used six and Kitahara et al. [9] used nine. To the best of our knowledge, the LEDs included in these systems were also selected based on maximizing the coverage of the visible light spectrum according to LED availability, without specifically considering color rendition.

Individual multispectral light sources have also been built [4, 8, 12, 13, 14] for image-based spectral reflectance measurements of scenes and materials. Park et al. [12] estimated scene reflectance spectra by capturing a sequence of images under RGYAW LED time-multiplexed multispectral illumination. Optimal combinations of these five LEDs were selected for each sequential illumination condition in the imaging system, but the initial selection of LEDs was not discussed. Parmer et al. [13] used RGYCA LEDs for multispectral imaging; Goel et al. [4] used 17 LEDs of distinct spectra for hyperspectral imaging (with 12 LEDs in the visible wavelength range), and Kimachi et al. [8] also used 12 different LEDs. However, optimal LED selections for reflectance measurements were not discussed. Shrestha et al. [14] described a multispectral LED-based imaging system, starting with a total of 19 LEDs of distinct spectra and generating optimal sets of three LEDs each, based on the accuracy of per-pixel estimated reflectance spectra or colors from either two or three photographs under sequential multispectral illumination conditions. While this approach is the most similar to ours, our objective differs in that we optimize LED selections for color rendition rather than spectral estimation, and we seek only one multispectral illumination condition for a single photograph while using any number of LEDs of distinct spectra.

Commercial Luminaire Design

While we primarily envision our multispectral light source used in an omnidirectional lighting rig designed for live-action compositing, as in prior works describing lighting reproduction [2, 6, 10], we also note that light sources with individually-controllable spectral channels may also be used in other professional studio lighting or consumer electronics contexts. In particular we note the availability of multispectral professional studio luminaires, such as the RGBW LED ARRI Skypanel and various RGBW and RGBA ColorKinetics LED light sources, as well as the consumer-focused Philips Hue LED light bulbs, which are three-channel Red, Lime, Royal Blue (RLY) or RGB luminaires. While the process of selecting the LEDs comprising these luminaires would be of theoretical interest to our work, to the best of our knowledge these manufacturers have not published technical motivations for these choices, besides the claims of being able to produce white light with varied and controllable correlated color temperatures (CCT).

Methods and Equations

Wenger et al. [16] described three optimization approaches for evaluating the performance of lighting reproduction systems. In this section, we summarize them and describe their applicability to computing an optimal combination of LEDs for multispectral lighting reproduction. For each possible LED combination, we solve for relative spectral channel intensities α_k using these approaches, and we then evaluate the color rendition performance using the accumulated error from each optimization approach. We seek to reproduce lighting with only positive spectra, so we obtain $\alpha_k \geq 0$ for all k by using nonnegative least squares.

Throughout our analysis, we assume a spectral camera model, with pixel values p_j generated by integrating over all wavelengths the modulation of an illuminant spectrum $I(\lambda)$ by the reflectance spectrum $R(\lambda)$ of a material, by the camera spectral sensitivity w_j for the observer's jth color channel:

$$p_j = \int_\lambda I(\lambda)R(\lambda)w_j(\lambda) \tag{1}$$

We compute pixel values using a discrete approximation of Eq. 1, where i is the index over the wavelength samples, dictated by measurement spectral resolution:

$$p_j = \sum_i I_i R_i w_{j,i} \tag{2}$$

1. Spectral Illuminant Matching

Using *Spectral Illuminant Matching* (SIM), the goal is to directly match a target illumination spectrum. We compute a linear combination of individual LED emission spectra that best matches a target illuminant spectrum in a least-squares sense. If two illuminants have the same spectra, then they will produce identical color appearances for all materials as seen by all observers. While this method maintains the observer-independence of LED selection, Wenger et al. [16] demonstrated for a nine-channel multispectral light source that SIM yielded the poorest color rendition of the various approaches. Finding the relative spectral channel intensities α_k given a target illuminant spectrum I is formulated as a least squares problem, considering the kth LED with emission spectrum I_k:

$$\text{argmin}(\sum_i(\sum_k \alpha_k I_{k,i} - I_i)^2) \mid \alpha_k \geq 0 \,\forall\, k \tag{3}$$

2. Metameric Illuminant Matching

Using *Metameric Illuminant Matching* (MIM), the goal is to match the *color* rather than the *spectrum* of a target illuminant, which requires knowledge or assumptions about the spectral sensitivity functions of the observer. Generating light that is metameric to a target illuminant only ensures that materials with spectrally-flat, neutral reflectance spectra will appear the same color under both illuminants to the target observer. Producing metameric light is also formulated as a least-squares problem, where w_j represents the spectral sensitivity of the observer's jth color channel:

$$\text{argmin}(\sum_j(\sum_i w_{j,i}\sum_k \alpha_k I_{k,i} - \sum_i I_i w_{j,i})^2) \mid \alpha_k \geq 0 \,\forall\, k \tag{4}$$

3. Metameric Reflectance Matching

As the goal of a lighting reproduction system is color rendition, *Metameric Reflectance Matching* (MRM) seeks to directly optimize the relative LED weights α_k for a multispectral light source to best match color appearances, for particular materials of interest, with known or measured reflectance spectra, and observer(s) with spectral sensitivities w_j. For n materials with known reflectance spectra R_n, producing light that affords material color matches is again formulated as a least-squares problem:

$$\text{argmin}(\sum_n\sum_j(\sum_i R_{n,i}w_{j,i}\sum_k \alpha_k I_{k,i} - \sum_i R_{n,i}I_i w_{j,i})^2) \mid \alpha_k \geq 0 \,\forall\, k \tag{5}$$

For MIM, the modulation of a target illuminant by the spectral sensitivities of one tristimulus observer yields only three equations, so we can theoretically only solve for optimal weights α_k for three-channel light sources. However, Wenger et al. [16] found a minimum norm, positive solution for a nine-channel source. Rather than solve this under-constrained MIM problem, we instead observe that the MIM constraints may be included in the MRM solve if a material with a flat reflectance spectrum, such as any neutral grayscale square of a color chart, is included. Such a spectrum modulates the incident illumination spectrum only by an overall, wavelength-independent scale factor. Similarly, if we sought to include SIM constraints in the MRM solve, we could design a set of theoretical reflectance spectra as pulse functions at increments equivalent to our measurement resolution (10 nm). Minimizing MRM error using a set of such functions is equivalent to minimizing SIM error.

Figure 3. *Circuit board with 11 LEDs of distinct spectra (some duplicates).*

Datasets

Towards an observer-agnostic optimal LED selection, we evaluate MRM color error for various LED combinations by using a database of spectral sensitivity functions for 28 cameras [7] and include the CIE 1931 2° standard observer. For test illuminants, we consider CIE illuminant A (tungsten lighting), D65 (average daylight), and F4 (fluorescent, used for calibrating the CIE

color rendering index, with CRI = 51). Since light sources of a light stage frequently reproduce indirect illumination, we also consider D65 modulated by measured reflectance spectra of grass and sand from the USGS Digital Spectral Library (SPLIB06a). We use these materials because of their frequent occurrence in natural scenes, but other materials may be of interest, depending on the lighting environment. We also consider diffuse skylight, which we measured at midday using a Photo Research PR-650 spectroradiometer. We use the 24 reflectance spectra of the X-Rite ColorChecker^{TM} chart for MRM. We also evaluate MRM color error for different skin tones using a database of 120 skin reflectance spectra, with measurements from the forehead and cheeks of 40 subjects [15]. As the spectral resolution and sampling extent vary across datasets, we resample each spectrum with trapezoidal binning between 400 and 700 nm to the coarsest resolution, 10 nm. As camera spectral sensitivity functions are typically broad, re-sampling error should be small. We affix each LED onto a custom circuit board (Fig. 3) and measure the emission spectra (Fig. 2) using the PR-650 spectroradiometer.

Results

Spectral Illuminant Matching

Fig. 4 shows the SIM sum of squared errors (SSE) (400-700 nm) for the normalized test illuminants, for several LED combinations. Optimal weights α_k are determined for each LED combination for each illuminant. We report the theoretical error using all 11 LEDs, the minimal error combinations of six and five LEDs, RGBW, and RGB only. As there are 462 combinations of six LEDs to construct from 11 LEDs, we always include RGBW in our sets of five or six LEDs, as these are useful for other light stage applications such as high resolution facial scanning. We therefore evaluate 21 LED combinations, varying two LEDs of a six-channel source.

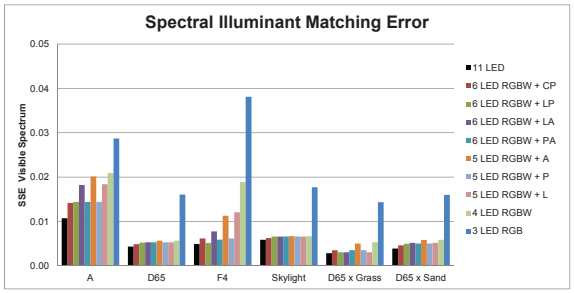

Figure 4. *Spectral Sum of Squared Errors, 400-700 nm, using SIM for six different illuminants, for various combinations of LEDs.*

The black bars of Fig. 4 represent the theoretically minimal SSE when using all 11 LEDs of distinct spectra. D65, Skylight, and the D65 modulated spectra are reproduced comparably with 4 (RGBW) and 11 LEDs. The five-channel RGBWP solve reproduces illuminants A and F4 comparably to the 11-channel solve.

Metameric Reflectance Matching

Fig. 5 shows the theoretical MRM average error for computed tristimulus values of the color chart, relative to the white square values. For each LED combination, we solve for optimal weights α_k for each observer separately and report the average color error across the 24 chart squares and the 29 observers (28 cameras and human observer). Therefore, we constrain that the LEDs used must be consistent across observers, but the LED intensities α_k may vary from observer to observer.

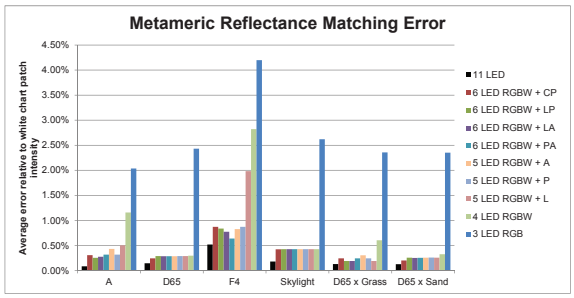

Figure 5. *Average squared error of tristimulus values from all 24 color chart squares for six different illuminants, using Metameric Reflectance Matching. Each bar represents the average error across 29 observers.*

Five-channel RGBWA and RGBWP solves again have similar error to the full 11-channel solve for MRM, with average error under 0.5% for illuminants A, D65, Skylight, and the D65 modulated spectra, and under 1% for illuminant F4. For a given LED arrangement and illuminant, average color errors for various observers are similar.

Although the reflectance spectra of the color chart are designed to replicate various real-world material spectra [11], skin tones are of particular interest for lighting reproduction. Fig. 6 shows the theoretical average MRM color error for 120 skin tones, corresponding to the forehead and cheek reflectance spectra from 40 subjects [15], relative to color chart white square values. For Fig. 6, we solve for optimal LED intensities α_k using only the 24 color checker reflectance spectra for MRM but independently report error for skin spectra (not included in the minimization).

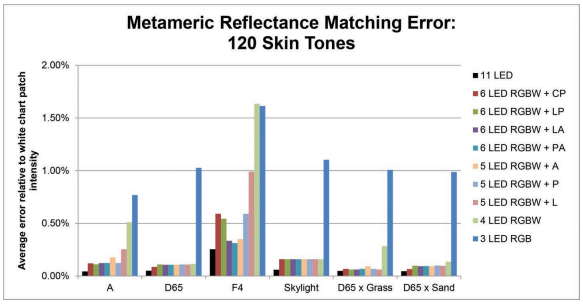

Figure 6. *Average squared error of tristimulus values computed from 120 skin reflectance spectra for six different illuminants, using Metameric Reflectance Matching solves from Fig. 5. Each bar represents the average error across 29 observers.*

We also separately solve for optimal LED intensities α_k when including these 120 spectra in the optimization, which reduces average skin tone color error to under 1% even for RGB-only lighting for each illuminant at the expense of increased color error for the color chart squares. The color rendition for the color chart squares is 0.1% worse on average and at most 0.6% worst, adding to the errors presented in Fig. 5.

Notably, SIM and MRM each produce an identical optimal set of five LEDs (RGBWP) for the illuminants and observers considered, and both error metrics show diminishing returns for spec-

tral matching or color rendition when including more than five spectral channels in a light source.

While for the experiments presented in Fig. 5 we tailor the light intensities α_k to each observer, we also solve for *one optimal set of intensities* α_k for each illuminant for *all observers* and again report the average error across all chart squares and observers. Fig. 7 shows the theoretical difference in the MRM color error as a function of the solving method (SIM, all-observers MRM, single-observer MRM). The single-observer MRM solves yield lower color error than the all-observer MRM solves, but the all-observer MRM error is still low, owing to the general similarity of camera spectral sensitivity functions.

For all illuminants and LED configurations, SIM yields more color error than even the all-observer MRM, indicating that lighting reproduction may benefit from a generic assumption about spectral sensitivity functions in the absence of measured observer response.

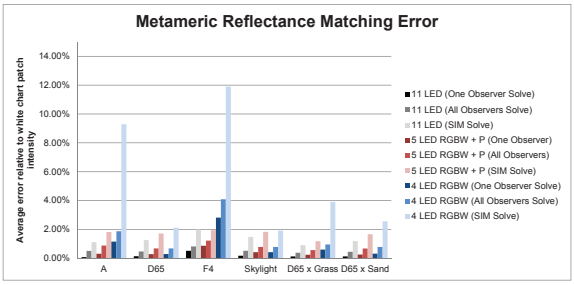

Figure 7. *Average squared error of tristimulus values from all 24 color chart squares for six different illuminants, using SIM, MRM (single-observer), and MRM (all-observers). Each bar represents the average error across 29 observers.*

We also present qualitative results for color rendition using the color chart MRM for the six illuminants for the CIE 2° standard observer in Fig. 8. The background squares represent the ground truth color chart appearances under the six illuminants, and the foreground circles represent the color chart appearances as illuminated by the MRM optimized lighting reproduction using 11 LEDs, RGBWP, RGBW, and RGB-only. All pixel values are computed using Eq. 2, and the XYZ tristimulus values are converted to sRGB for display. RGBW lighting produces visually accurate color rendition for illuminants D65, Skylight, and D65 modulated by grass and sand reflectance spectra. Adding the PC Amber LED yields visually accurate color rendition for the remaining illuminants, A and F4.

In Fig. 9, we compare the spectra from the human observer color chart MRM lighting reproduction with 11 LEDs, RGBWP, RGBW, and RGB-only with the six ground truth illuminant spectra re-sampled at 10 nm resolution (solid black lines). The spectra of Fig. 9 therefore correspond to those used to generate the color charts of Fig. 8. While the reproduced lighting spectra do not exactly match the ground truth illuminant spectra, even with 11 spectral channels, the LED reproduced lighting still yields close visual matches (Fig. 8).

Using the optimal LED intensities α_k computed for the CIE 2° standard observer color charts of Fig. 8, we also present qualitative results for color rendition for a selection of 24 skin reflectance spectra in Fig. 10. These 24 spectra were selected from the original set of 120 so as to evenly cover the possible values for total light reflected across the visible spectrum. Again, background squares represent the ground truth skin appearances under the six illuminants, and foreground circles represent appearances as illuminated by the MRM optimized lighting reproduction using 11 LEDs, RGBWP, RGBW, and RGB-only. RGBW lighting produces visually accurate color rendition for illuminants A, D65, Skylight, and D65 modulated by the sand reflectance spectrum. Adding the PC Amber LED yields visually accurate color rendition for the remaining illuminants, F4 and D65 modulated by grass reflectance spectrum.

Future Work

The experiments of this work describe the theoretically achievable color rendition capabilities of various combinations of LEDs, considering specific illuminants, materials, and observers. While we have shown that a five-channel RGBWP light source should be theoretically sufficient for multispectral lighting reproduction, it would be interesting to validate these results with physical measurements, to compare theoretical and experimental error as in prior work [16, 10]. Such a validation would require the physical existence of particular illuminants, and so the direct image-based MRM optimization approach of LeGendre et al. [10] could be employed, which does not rely on spectral measurements.

Additionally, visual effects practitioners may have particular interest in digital cinema cameras such as the RED Epic and the ARRI Alexa, which were not included in the camera database [7]. The same optimization approaches could be applied to ensure the optimal LED selection for these cameras if their spectral sensitivities were known or measured. Without knowledge of the camera spectral response, the image-based MRM minimization approach [10] could again be employed.

While our optimization approach did not evaluate the overall brightness of the light produced by each combination of LEDs for a given power input, it is well known that LEDs of different spectra have varied luminous efficiency. Future work could optimize for luminous efficiency in tandem with color rendition performance and identify potential trade-offs between these goals.

Although multispectral lighting reproduction produces visually accurate color rendition without the need for color correction in post-production, camera raw pixel values produced by the sensor will inevitably have a color matrix applied to them for display as part of a typical color workflow. A 3×3 color matrix allows for linear color channel mixing, in effect producing a different theoretical camera sensor. Another direction for future work could include optimizing LED selection based on both luminous efficiency and color rendition performance, while allowing for a post-processing color matrix step.

Conclusion

We have demonstrated that material color appearance under various direct and indirect illuminants may be accurately matched using as few as five LEDs of distinct spectra for multispectral lighting reproduction: red, green, blue, white, and broad-spectrum PC Amber. Using more than these five LEDs of distinct spectra yields diminishing returns. Spectral illuminant matching and color appearance matching via metameric reflectance yield the same optimal set of five LEDs for the illuminants and observers considered.

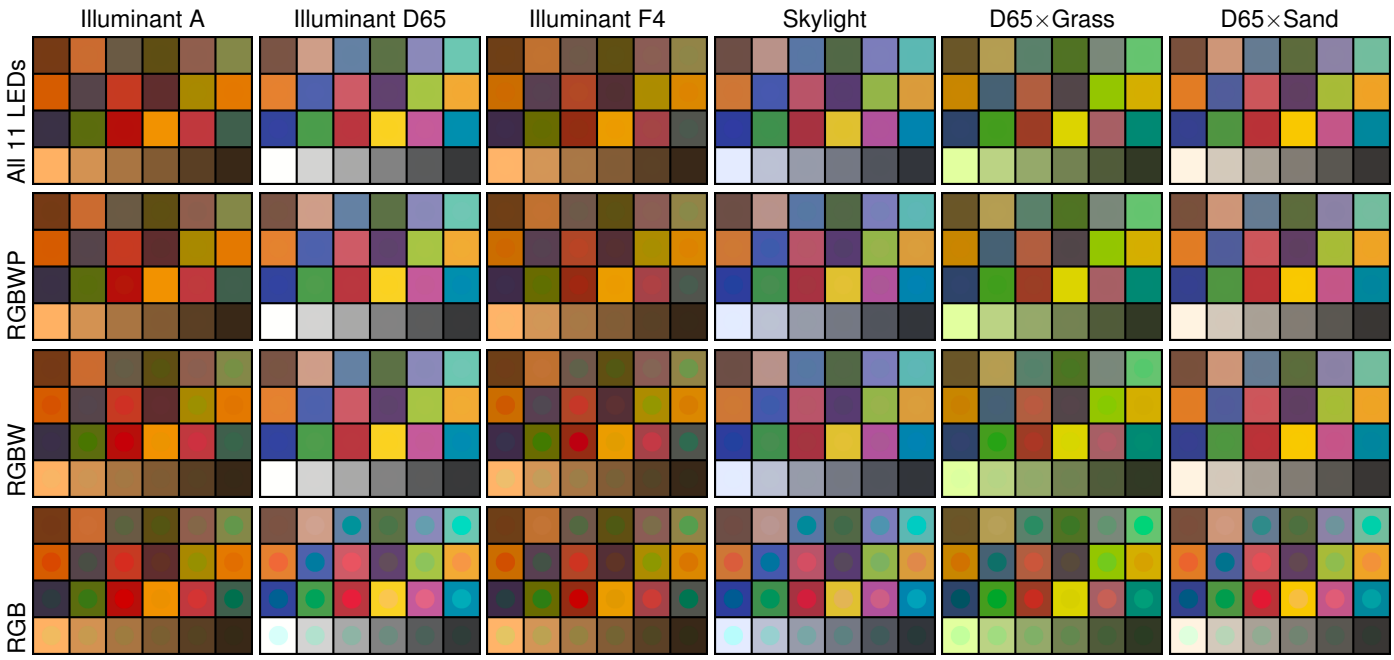

Figure 8. *Color matching results using Metameric Reflectance Matching for different direct and indirect illuminants for the CIE 2° standard observer, with illumination reproduced using various LED combinations. The background squares represent the ground truth computed color chart appearances under the target illuminants, while the foreground circles represent the computed color chart appearances under LED-reproduced illumination. Row 1 shows the lighting reproduction results using all 11 LEDs of distinct spectra. Row 2 shows results using 5 LEDs only (RGB, White and PC Amber). Row 3 shows results using RGBW only. Row 4 shows the result using RGB only. XYZ tristimulus values are converted to the sRGB color space for display. RGBW lighting produces accurate color rendition for D65, Skylight, and D65 modulated by grass and sand reflectance spectra. Adding PC Amber yields accurate color rendition for illuminants A and F4.*

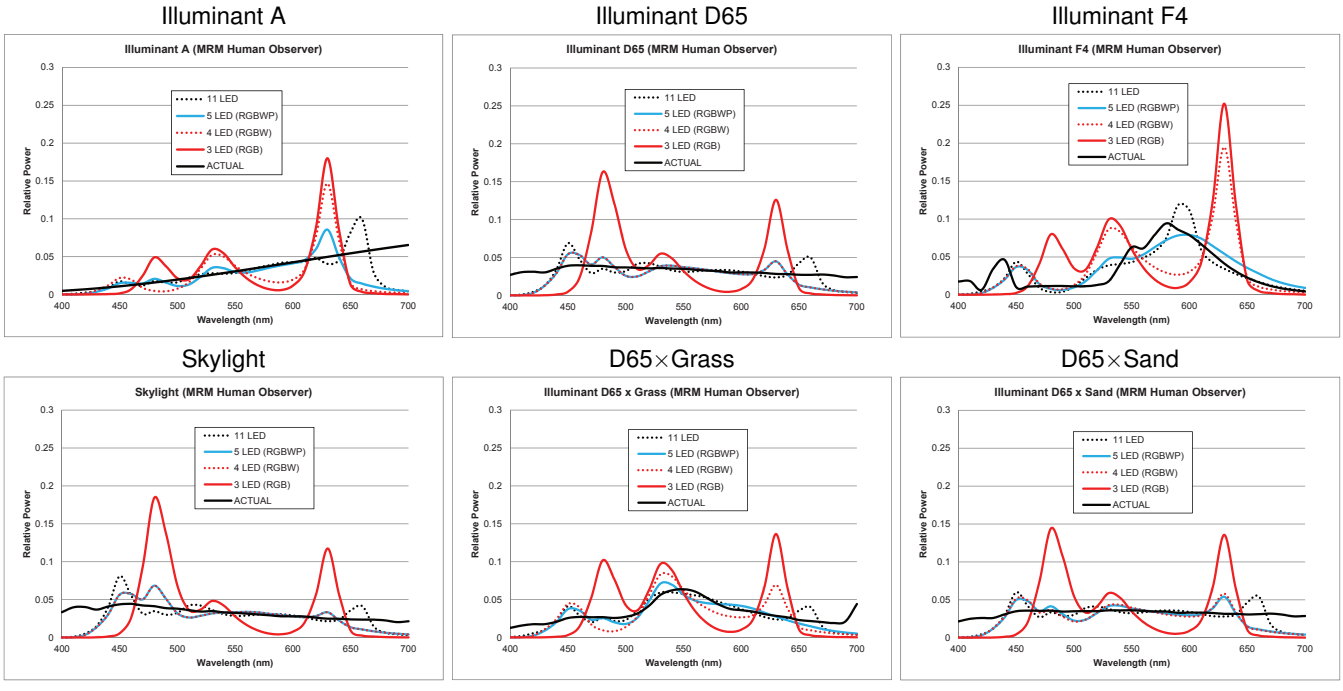

Figure 9. *Spectra produced using Metameric Reflectance Matching for different direct and indirect illuminants for the CIE 2° standard observer, using various LED combinations. Solid black lines represent the ground truth illuminant spectra re-sampled at 10 nm resolution.*

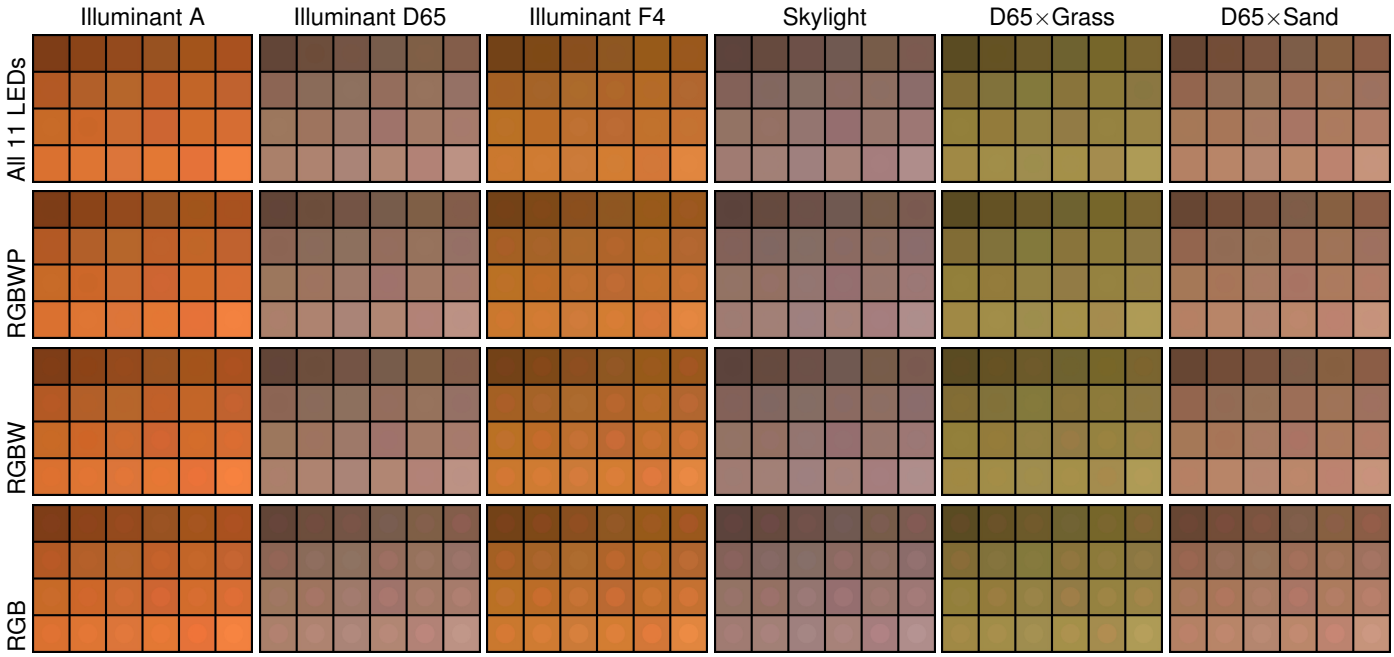

Figure 10. *Color matching results using Metameric Reflectance Matching for different direct and indirect illuminants for the CIE 2° standard observer, with illumination reproduced using various LED combinations. The background squares represent the ground truth computed skin tone appearances under the target illuminants, while the foreground circles represent the computed skin tone appearances under LED-reproduced illumination. Row 1 shows the lighting reproduction results using all 11 LEDs of distinct spectra. Row 2 shows results using 5 LEDs only (RGB, White and PC Amber). Row 3 shows results using RGBW only. Row 4 shows the result using RGB only. XYZ tristimulus values are converted to the sRGB color space for display. RGBW lighting produces accurate color rendition for A, D65, Skylight, and D65 modulated by the sand reflectance spectrum. Adding PC Amber yields accurate color rendition for illuminants F4 and D65 modulated by the grass reflectance spectrum.*

Acknowledgments

The authors wish to thank Randy Hill, Kathleen Haase, Christina Trejo, Jay Busch, Andrew Jones, Shanhe Wang, Kathryn Rock, and the Natick Soldier Systems Center for their important support of this work. This project was sponsored by the U.S. Army Research Laboratory (ARL) under contract W911NF-14-D-0005 and in part by a USC Annenberg Ph.D. Fellowship. The content of the information does not necessarily reflect the position or the policy of the Government, and no official endorsement should be inferred.

References

[1] B. Ajdin, M. Finckh, C. Fuchs, J. Hanika, and H. Lensch. Compressive higher-order sparse and low-rank acquisition with a hyperspectral light stage. Technical report, Univ. of Tuebingen, 2012.

[2] P. Debevec, A. Wenger, C. Tchou, A. Gardner, J. Waese, and T. Hawkins. A lighting reproduction approach to live-action compositing. In *Proc. 29th Annual Conference on Computer Graphics and Interactive Techniques*, SIGGRAPH '02, pages 547–556, New York, NY, USA, 2002. ACM.

[3] I. Fryc, S. W. Brown, and Y. Ohno. Spectral matching with an led-based spectrally tunable light source. In *Optics & Photonics 2005*, pages 59411I–59411I. International Society for Optics and Photonics, 2005.

[4] M. Goel, E. Whitmire, A. Mariakakis, T. S. Saponas, N. Joshi, D. Morris, B. Guenter, M. Gavriliu, G. Borriello, and S. N. Patel. Hypercam: hyperspectral imaging for ubiquitous computing applications. In *Proceedings of the 2015 ACM International Joint Conference on Pervasive and Ubiquitous Computing*, pages 145–156. ACM, 2015.

[5] J. Gu and C. Liu. Discriminative illumination: Per-pixel classification of raw materials based on optimal projections of spectral brdf. In *Computer Vision and Pattern Recognition (CVPR), 2012 IEEE Conference on*, pages 797–804, June 2012.

[6] P.-L. Hamon, J. Harmer, S. Penn, and N. Scapel. Gravity: Motion control and face integration. In *ACM SIGGRAPH 2014 Talks*, SIGGRAPH '14, pages 35:1–35:1, New York, NY, USA, 2014. ACM.

[7] J. Jiang, D. Liu, J. Gu, and S. Susstrunk. What is the space of spectral sensitivity functions for digital color cameras. In *Applications of Computer Vision WACV, 2013 IEEE Workshop on*, pages 168–179, 2013.

[8] A. Kimachi, H. Ikuta, Y. Fujiwara, M. Masumoto, and H. Matsuyama. Spectral matching imager using amplitude-modulation-coded multispectral light-emitting diode illumination. *Optical engineering*, 43(4):975–985, 2004.

[9] M. Kitahara, T. Okabe, C. Fuchs, and H. Lensch. Simultaneous estimation of spectral reflectance and normal from a small number of images. In *Proceedings of the 10th International Conference on Computer Vision Theory and Applications*, VISAPP 2015, pages 303–313, 2015.

[10] C. LeGendre, X. Yu, D. Liu, J. Busch, A. Jones, S. Pattanaik, and P. Debevec. Practical multispectral lighting reproduction. *ACM Trans. Graph.*, 35(4), July 2016.

[11] C. McCamy, H. Marcus, and J. Davidson. A color-rendition chart.

Journal of Applied Photographic Engineering, 2(3):95–99, June 1976.

[12] J.-I. Park, M.-H. Lee, M. D. Grossberg, and S. K. Nayar. Multispectral imaging using multiplexed illumination. In *2007 IEEE 11th International Conference on Computer Vision*, pages 1–8. IEEE, 2007.

[13] M. Parmar, S. Lansel, and J. Farrell. An led-based lighting system for acquiring multispectral scenes. In *IS&T/SPIE Electronic Imaging*, pages 82990P–82990P. International Society for Optics and Photonics, 2012.

[14] R. Shrestha and J. Y. Hardeberg. Multispectral imaging using led illumination and an rgb camera. In *Color and Imaging Conference*, volume 2013, pages 8–13. Society for Imaging Science and Technology, 2013.

[15] M. Uzair, A. Mahmood, F. Shafait, C. Nansen, and A. Mian. Is spectral reflectance of the face a reliable biometric? *Optics Express*, 23(12):15160–15173, 2015.

[16] A. Wenger, T. Hawkins, and P. Debevec. Optimizing color matching in a lighting reproduction system for complex subject and illuminant spectra. In *Proceedings of the 14th Eurographics Workshop on Rendering*, EGRW '03, pages 249–259, Aire-la-Ville, Switzerland, 2003. Eurographics Association.

Author Biography

Chloe LeGendre received a B.S. in Engineering in 2009 from the University of Pennsylvania and a M.S. in Computer Science from the Stevens Institute of Technology in 2015. From 2011 to 2015, she was an applications technologist in imaging and augmented reality for L'Oreal Research. She is currently pursuing a Ph.D. in Computer Science at the University of Southern California's Institute for Creative Technologies, advised by Professor Paul Debevec.

Xueming Yu received a B.S. in Electrical Engineering from Shanghai Jiao Tong University in 2005 and an M.S. degree in Computer Science from the University of Southern California in 2010. He developed 3D display technologies at Sony Corporation R&D and the electronics and mechanics for several Light Stage and surface reflectance scanning systems at the USC Institute for Creative Technologies. In 2016 he joined Google VR as a Hardware Engineer.

Paul Debevec received a Ph.D. in Computer Science from the University of California, Berkeley in 1996 under Professor Jitendra Malik specializing in photogrammetry and image-based rendering, with postdoctoral work in High Dynamic Range Imaging, Image-Based Lighting, and Reflectance Field capture. Light Stage systems from his laboratory at the USC Institute for Creative Technologies have been used to digitize models of actors in numerous feature films and were recognized with an Academy Scientific and Engineering Award in 2010. In 2016 he joined Google VR as a Senior Staff Engineer. http://www.debevec.org/